

## THERMAL STABILITY AND NONISOTHERMAL DECOMPOSITION KINETIC STUDY OF SOME COORDINATION COMPOUNDS OF Ni<sup>(II)</sup> AND Co<sup>(II)</sup>

MIHAELA BADEA and DANA MARINESCU

*Department of Inorganic Chemistry and Technology, Faculty of Chemical Technology,  
Polytechnical Institute of Bucharest, str. Dumbraava Roşie 23, Bucharest (Romania)*

E. SEGAL

*Department of Physical Chemistry and Electrochemical Technology, Faculty of Chemical Tech-  
nology, Polytechnical Institute of Bucharest, Bulevardul Republicii 13, Bucharest (Romania)*

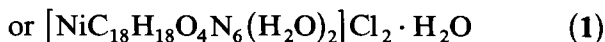
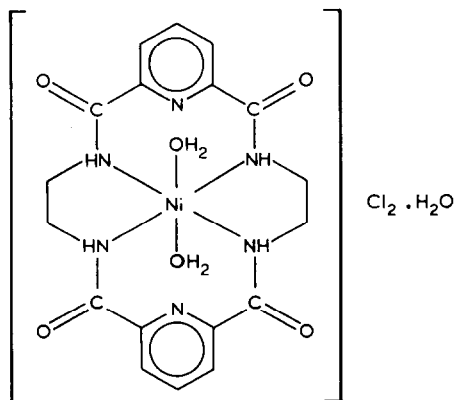
(Received 14 December 1988)

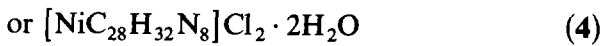
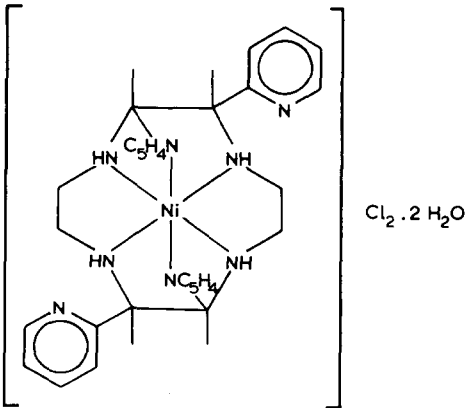
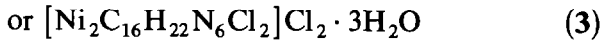
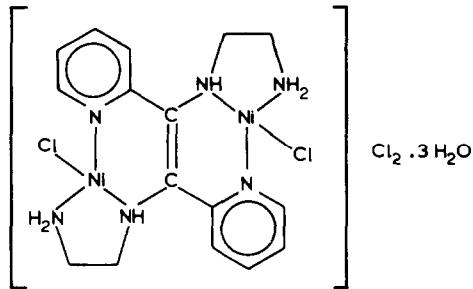
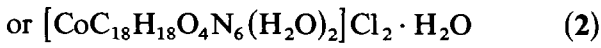
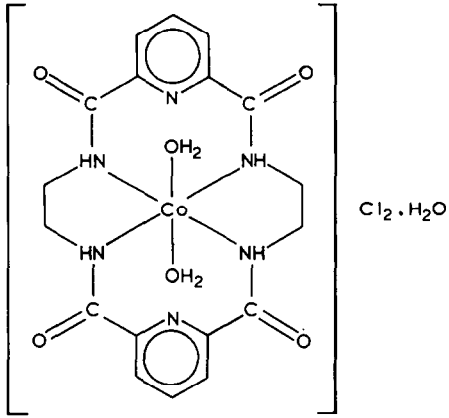
### ABSTRACT

The authors present some data concerning the thermal stability of four coordination compounds of Ni<sup>(II)</sup> and Co<sup>(II)</sup>. The non-isothermal kinetic parameters of the heterogeneous decomposition have been evaluated using three methods which gave results in satisfactory agreement. The data have been processed using original computer programs.

### INTRODUCTION

Following our research concerning the thermal stability of the coordination compounds [1], this paper deals with the following substances





## EXPERIMENTAL

### *Materials*

The compounds 1–4 were synthesized and analysed according to methods previously described [2].

### *Equipment*

The heating curves (TG, DTG, DTA) of the powdered samples were recorded in static air atmosphere between room temperature and 1000 °C for various heating rates between 2 and 10 K min<sup>-1</sup>, using an MOM Budapest, Paulik–Paulik–Erdey-type derivatograph.

X-ray diffractograms of the investigated samples were obtained using a Philips P.W. 1140 diffractometer and Cr  $K\alpha$  radiation.

The IR spectra were obtained with a Zeiss–Jena, Specord IR-71 spectrophotometer.

Chemical analysis was used to confirm the structures of some of the intermediates.

### *Analysis of the experimental data*

The mean crystallite sizes of the powders were determined from the X-ray diffractograms using Scherrer's formula [3].

In order to calculate the values of the non-isothermal kinetic parameters, three methods, according to Coats–Redfern [4], Flynn–Wall [5] for constant heating rate and Coats–Redfern modified by Urbanovici and Segal [6], were applied.

The experimental data were automatically analysed using the following BASIC programs run on a TIM-S personal computer: two programs for the Coats–Redfern method and the Flynn–Wall method for constant heating rate [7,8], a program written by Coseac and Segal for the modified Coats–Redfern method [9] and a program written by Coseac and Segal to regenerate the TG curves in the  $\alpha$  and  $T$  (°C) coordinates using the non-isothermal kinetic parameters evaluated by the Coats–Redfern method [10].

## RESULTS AND DISCUSSION

### *The X-ray diffractograms and mean crystallite sizes*

The interplanar distances  $d$  (Å), the relative intensities of the diffraction lines and the crystallite sizes  $l$  (Å) for the investigated compounds are given in Tables 1–3.

TABLE 1

Interplanar distances, relative intensities of the diffraction lines and crystallite mean sizes of  $[\text{NiC}_{18}\text{H}_{18}\text{O}_4\text{N}_6(\text{H}_2\text{O})_2]\text{Cl}_2 \cdot \text{H}_2\text{O}$

| $d$ (Å) | Relative intensity | $l$ (Å) |
|---------|--------------------|---------|
| 3.46    | 78                 |         |
| 3.34    | 70                 |         |
| 3.27    | 65                 |         |
| 2.99    | 100                | 320     |
| 2.63    | 50                 |         |

TABLE 2

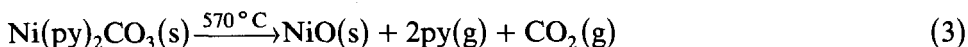
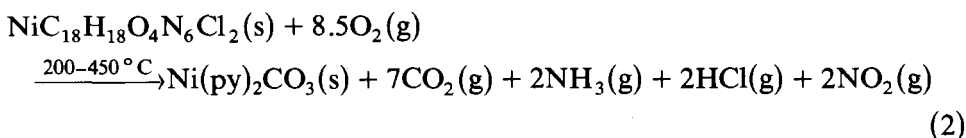
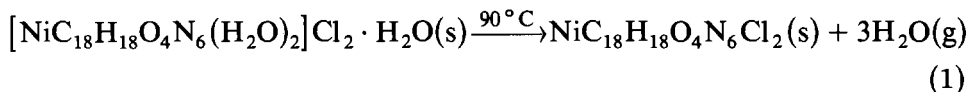
Interplanar distances, relative intensities of the diffraction lines and crystallite mean sizes of  $[\text{CoC}_{18}\text{H}_{18}\text{O}_4\text{N}_6(\text{H}_2\text{O})_2]\text{Cl}_2 \cdot \text{H}_2\text{O}$

| $d$ (Å) | Relative intensity | $l$ (Å) |
|---------|--------------------|---------|
| 3.44    | 90                 |         |
| 3.34    | 81                 |         |
| 3.23    | 60                 |         |
| 3.02    | 100                | 310     |
| 2.63    | 50                 |         |

For  $[\text{Ni}_2\text{C}_{16}\text{H}_{22}\text{N}_6\text{Cl}_2]\text{Cl}_2 \cdot 3\text{H}_2\text{O}$ , the diffractogram exhibits only one line corresponding to  $d = 3.02$  Å and  $l = 315$  Å.

*The decomposition of  $[\text{NiC}_{18}\text{H}_{18}\text{O}_4\text{N}_6(\text{H}_2\text{O})_2]\text{Cl}_2 \cdot \text{H}_2\text{O}$*

According to the TG curve (Fig. 1), this compound undergoes decomposition in the following steps



In eqns. (1) and (3) and in other similar equations, the temperatures written above the arrows correspond to the maximum decomposition rate, according to the DTG curve. As far as reaction (2) is concerned, this occurs in several steps which are difficult to separate, in the temperature interval 200–450°C.

TABLE 3

Interplanar distances, relative intensities of the diffraction lines and crystallite mean sizes of  $[\text{NiC}_{28}\text{H}_{32}\text{N}_8]\text{Cl}_2 \cdot 2\text{H}_2\text{O}$

| $d$ (Å) | Relative intensity | $l$ (Å) |
|---------|--------------------|---------|
| 7.15    | 72                 |         |
| 6.92    | 72                 |         |
| 6.71    | 57                 |         |
| 6.39    | 68                 |         |
| 4.82    | 13                 |         |
| 4.43    | 75                 |         |
| 4.28    | 100                | 172     |
| 3.93    | 70                 |         |
| 3.70    | 47                 |         |
| 3.38    | 23                 |         |
| 3.29    | 32                 |         |
| 3.16    | 53                 |         |
| 3.08    | 13                 |         |
| 2.98    | 17                 |         |
| 2.95    | 21                 |         |
| 2.69    | 17                 |         |
| 2.48    | 21                 |         |
| 2.47    | 15                 |         |

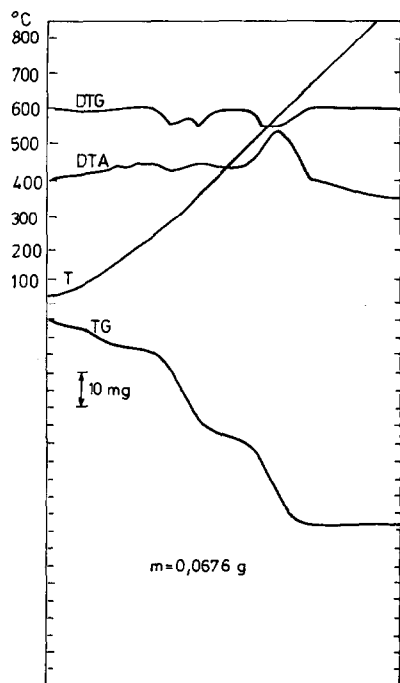


Fig. 1. The derivatogram of  $[\text{NiC}_{18}\text{H}_{18}\text{O}_4\text{N}_6(\text{H}_2\text{O})_2]\text{Cl}_2 \cdot \text{H}_2\text{O}(\text{s})$ .

TABLE 4

Values of the non-isothermal kinetic parameters of reaction (1) ( $\beta = 2.43 \text{ K min}^{-1}$ )

| Method                 | $n$ | $E$ (cal mol <sup>-1</sup> ) | $A$ (s <sup>-1</sup> ) |
|------------------------|-----|------------------------------|------------------------|
| Coats-Redfern          | 2.3 | $1.2 \times 10^4$            | $8.44 \times 10^3$     |
| Flynn-Wall             | 2.3 | $1.3 \times 10^4$            | $9.90 \times 10^3$     |
| Modified Coats-Redfern | 2.3 | $1.14 \times 10^4$           | $6.77 \times 10^3$     |

TABLE 5

Values of the non-isothermal kinetic parameters of reaction (3) ( $\beta = 2.43 \text{ K min}^{-1}$ )

| Method                 | $n$ | $E$ (cal mol <sup>-1</sup> ) | $A$ (s <sup>-1</sup> ) |
|------------------------|-----|------------------------------|------------------------|
| Coats-Redfern          | 1.7 | $5.43 \times 10^4$           | $1.25 \times 10^{12}$  |
| Flynn-Wall             | 1.7 | $5.46 \times 10^4$           | $1.57 \times 10^{12}$  |
| Modified Coats-Redfern | 1.6 | $5.32 \times 10^4$           | $5.94 \times 10^{11}$  |

The DTA curve exhibits an endothermic effect at  $\sim 190^\circ\text{C}$  without any change on the TG and DTG curves. This could be assigned to a transition from a square-planar coordination to a tetrahedral one. This change is reversible, as shown by the X-ray diffractogram, as is the colour change of the compound obtained at  $200^\circ\text{C}$  during cooling. The existence of  $\text{Ni}(\text{py})_2\text{CO}_3$  as a product of reaction (2) was confirmed by the IR spectrum, which exhibits the characteristic bands of carbonate and coordinate pyridine. The presence of  $\text{NiO}$ , the solid product of reaction (3), was confirmed on the X-ray diffractogram of the decomposition residue obtained above  $600^\circ\text{C}$ .

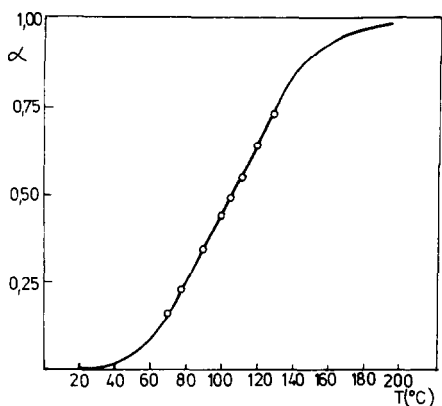


Fig. 2. Thermogravimetric curve in coordinates  $\alpha$  and  $T$  ( $^\circ\text{C}$ ) for reaction (1): — calculated curve,  $\circ$ , experimental points.

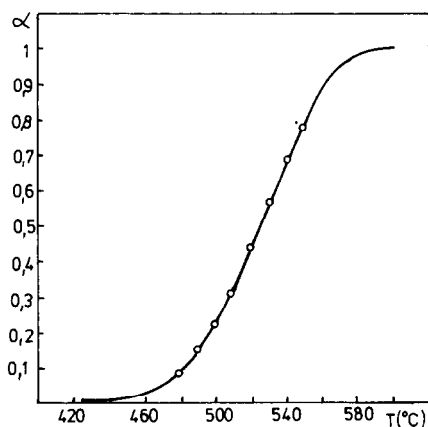


Fig. 3. Thermogravimetric curve in coordinates  $\alpha$  and  $T$  ( $^{\circ}\text{C}$ ) for reaction (3): — calculated curve,  $\circ$ , experimental points.

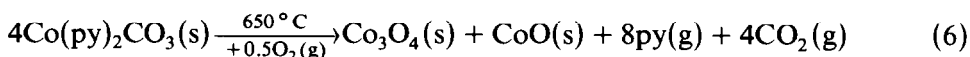
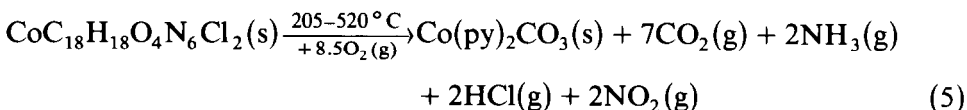
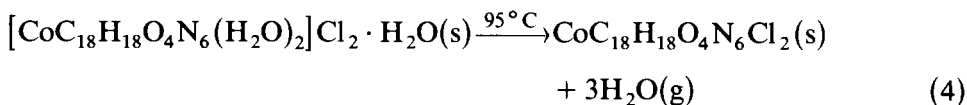
Tables 4 and 5 list the values of the non-isothermal kinetic parameters, the reaction order  $n$ , the activation energy  $E$ , and the pre-exponential factor  $A$  for reactions (1) and (3).

The relatively low heating rate ( $2.43 \text{ K min}^{-1}$ ) ensures that the reaction conditions are quite close to isothermal. Inspection of Tables 4 and 5 shows that the three methods applied gave results which are in satisfactory agreement.

Figures 2 and 3 show the plots of the regenerated TG curves for reactions (1) and (3). The Coats–Redfern non-isothermal kinetic parameters were used to plot the curves. From these figures, it can be seen that the experimental points fit well with the calculated curves.

#### *The decomposition of $[\text{CoC}_{18}\text{H}_{18}\text{O}_4\text{N}_6(\text{H}_2\text{O})_2]\text{Cl}_2 \cdot \text{H}_2\text{O}$*

According to the heating curves recorded between 20 and  $1000^{\circ}\text{C}$ , the decomposition occurs through the following steps



As in the former case, at  $210^{\circ}\text{C}$  the DTA curve exhibits the thermal effect corresponding to the square-planar–tetrahedral coordination transition. This transition is reversible. The colour change shown by the com-

TABLE 6

Values of the non-isothermal kinetic parameters of reaction (4) ( $\beta = 2.5 \text{ K min}^{-1}$ )

| Method                 | $n$ | $E \text{ (cal mol}^{-1}\text{)}$ | $A \text{ (s}^{-1}\text{)}$ |
|------------------------|-----|-----------------------------------|-----------------------------|
| Coats-Redfern          | 2.2 | $1.58 \times 10^4$                | $9.81 \times 10^6$          |
| Flynn-Wall             | 2.1 | $1.46 \times 10^4$                | $1.45 \times 10^6$          |
| Modified Coats-Redfern | 2.1 | $1.53 \times 10^4$                | $8.32 \times 10^6$          |

TABLE 7

Values of the non-isothermal kinetic parameters of reaction (6) ( $\beta = 2.22 \text{ K min}^{-1}$ )

| Method                 | $n$ | $E \text{ (cal mol}^{-1}\text{)}$ | $A \text{ (s}^{-1}\text{)}$ |
|------------------------|-----|-----------------------------------|-----------------------------|
| Coats-Redfern          | 0.3 | $1.72 \times 10^4$                | 6.74                        |
| Flynn-Wall             | 0.2 | $1.90 \times 10^4$                | $1.08 \times 10$            |
| Modified Coats-Redfern | 0.3 | $1.71 \times 10^4$                | $1.56 \times 10$            |

pound heated to  $210^\circ\text{C}$  with temperature decrease, as well as the X-ray diffractograms, confirm the reversibility of the transition. The IR spectrum confirms the existence of  $\text{Co(py)}_2\text{CO}_3$ . The X-ray diffractogram of the final solid decomposition product exhibits the lines of  $\text{Co}_3\text{O}_4$  as well as those of  $\text{CoO}$ .

The non-isothermal kinetic parameters of reactions (4) and (6) are listed in Tables 6 and 7.

These results show that for reactions (4) and (6), the methods applied to evaluate the non-isothermal kinetic parameters led to values which are in fairly satisfactory agreement.

Figure 4 shows the regenerated TG curve plotted using the Coats-Redfern non-isothermal kinetic parameters for reaction (4).

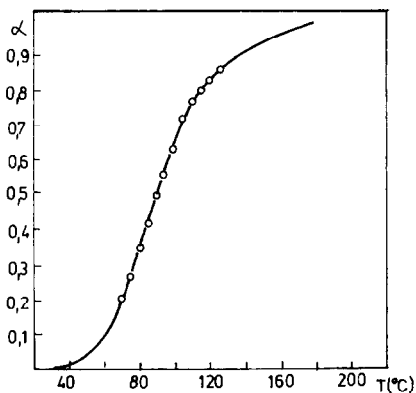
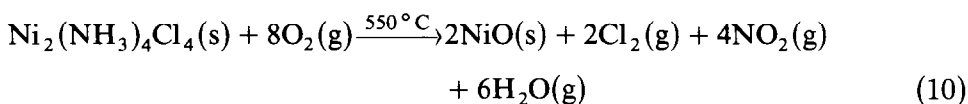
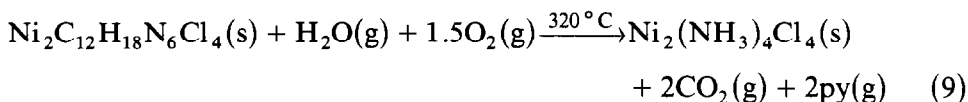
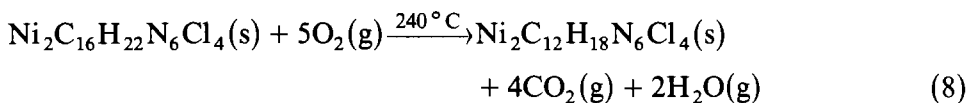
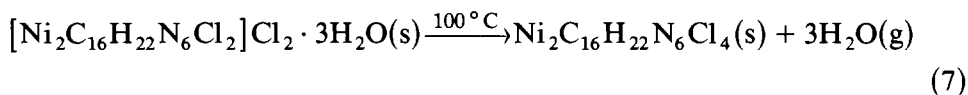


Fig. 4. Thermogravimetric curve in coordinates  $\alpha$  and  $T \text{ (}^\circ\text{C)}$  for reaction (4): —, calculated curve, O, experimental points.



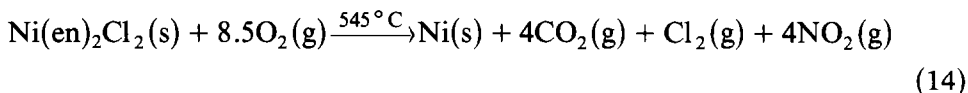
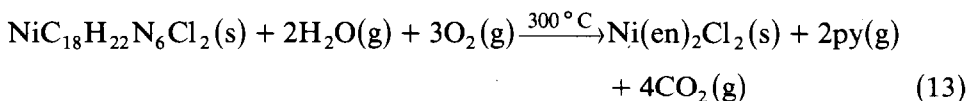
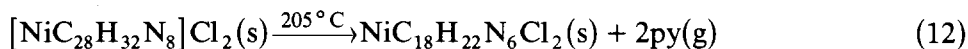
*The decomposition of  $[\text{Ni}_2\text{C}_{16}\text{H}_{22}\text{N}_6\text{Cl}_2]\text{Cl}_2 \cdot 3\text{H}_2\text{O}$*

According to the heating curves, this compound undergoes decomposition in the following steps



*The decomposition of  $[\text{NiC}_{28}\text{H}_{32}\text{N}_8]\text{Cl}_2 \cdot 2\text{H}_2\text{O}$*

The heating curves exhibited the following decomposition steps



As the DTG curve corresponding to reactions (7)–(14) shows that these are not simple reactions, non-isothermal kinetic analysis was not performed on them.

The fractional reaction order values, between 0 and 1, could be assigned to an intermediate regime (diffusional and kinetic) which controls the occurrence of a reaction [11]. For reaction order values higher than 1, these could be assigned to the decomposition of some structural units which consist of various, low numbers of molecules.

## CONCLUSIONS

The main decomposition steps through which the thermal decomposition of four coordination compounds of Ni(II) and Co(II) have been outlined.

For the simple decomposition steps, a non-isothermal kinetic analysis was performed. The values of the kinetic parameters obtained using three methods are in satisfactory agreement.

#### REFERENCES

- 1 E. Segal and D. Fătu, Introduction to Non-isothermal Kinetics, Publishing House of the Academy of Socialist Republic of Romania, Bucharest, 1983, p. 259 (in Romanian).
- 2 R. Olar, D. Marinescu and M. Andruh, unpublished work.
- 3 A. Guinier, *Théorie et Technique de la Radiocristallographie*, Dunod, Paris, 1964, p. 462.
- 4 A.W. Coats and J.P. Redfern, *Nature (London)*, 201 (1964) 68.
- 5 J.H. Flynn and L.A. Wall, *Polym. Lett.*, 41 (1966) 323.
- 6 E. Urbanovici and E. Segal, *Thermochim. Acta*, 80 (1984) 379.
- 7 T. Coseac and E. Segal, *Rev. Roum. Chim.* 34 (1989) 287.
- 8 M. Badea and E. Segal, unpublished work.
- 9 T. Coseac and E. Segal, unpublished work.
- 10 T. Coseac and E. Segal, unpublished work.
- 11 E. Segal, in V.V. Boldyrev and K. Meyer (Eds.), *Festkörperchemie*, VEB, Deutscher Verlag für Grundstoffindustrie, Leipzig, 1973, p. 404.